ATMOSPHERIC ENVIRONMENT: X 26 (2025) 100324

Contents lists available at ScienceDirect

Atmospheric Environment: X

journal homepage: www.journals.elsevier.com/atmospheric-environment-x

Cement and brick factories contribute elevated levels of NO_2 pollution in Nepal: Evidence of high-resolution view from space

Madhu S. Gyawali [a,*], Lok N. Lamsal [b,c,**], Sujan Neupane [d], Bimal Gyawali [e], Keshav Bhattarai [f], Bradford Fisher [g,c], Nickolay Krotkov [c], Jos van Geffen [h], Henk Eskes [h], Shriram Sharma [i], Cameron Brunt [a], Rudra Aryal [j]

[a] Undergraduate Research Center, San Jacinto College, South Campus, Houston, TX, 77089, USA
[b] Goddard Earth Sciences Technology and Research II, University of Maryland Baltimore County, Baltimore, MD, 21250, USA
[c] NASA Goddard Space Flight Center, Greenbelt, MD, 20771, USA
[d] Department of Computer Science and Electrical Engineering, University of Maryland Baltimore County, Baltimore, MD, 21250, USA
[e] Department of Earth and Atmospheric Science, University of Houston, Houston, TX, 77004, USA
[f] Department of Physical Sciences, University of Central Missouri, Warrensburg, MO, 64093, USA
[g] Science Systems and Applications, Inc. (SSAI), Lanham, MD, 20706, USA
[h] Royal Netherlands Meteorological Institute (KNMI), De Bilt, The Netherlands
[i] Department of Physics, Amrit Campus, Tribhuvan University, Kathmandu, Nepal
[j] Franklin Pierce University, Rindge, NH, 03461, USA

ARTICLE INFO

Keywords:
Nitrogen dioxide
Satellite
Air quality
Brick factory
Cement industry

ABSTRACT

An upsurge in the pollution level in areas with a high concentration of brick and cement factories in Nepal is concerning. Nitrogen dioxide (NO_2), a key air quality indicator, can be effectively monitored from space. This study utilizes high-resolution satellite observations of NO_2 from the TROPOspheric Monitoring Instrument (TROPOMI). It examines the NO_2 distribution over areas with emerging sources of nitrogen oxides from brick and cement factories from 2018 to 2021. Rapid growth of brick and cement factories has turned the Lumbini-Butwal-Palpa corridor, in Midwest Nepal, more polluted than the capital city Kathmandu. Between 2019 and 2021, NO_2 levels in this corridor rose considerably, while it remained steady in the Kathmandu Valley. TROPOMI-derived NO_2 levels and inferred NO_x emissions over the corridor nearly doubled in the span of three years. Conversely, Kathmandu Valley exhibited no significant changes except in 2020 when NO_2 and NO_x levels declined. This drop coincided with COVID-19-related travel restrictions and other reduced activities. NO_2 pollution recorded by the Ozone Monitoring Instrument (OMI) from 2005 to 2019 shows an annual NO_2 increase of ~3.5 % over both regions. A comparison between NO_x emissions from the 2018 EDGAR inventory and TROPOMI-derived estimates for 2019 reveal comparable values over the Lumbini-Butwal-Palpa corridor but around 35 % higher estimates over Kathmandu. This discrepancy over the capital city, as well as the rapid rise in emissions over the Lumbini-Butwal-Palpa corridor due to a large-scale development of cement and brick industries, highlights the need for timely updates in bottom-up emission inventory.

Plain summary

Satellite-based air quality sensors can monitor pollution sources and their emission strengths worldwide, complementing ground-based observations. Detection of emissions is easier for short-lived pollutants, such as nitrogen dioxide (NO_2), due to enhanced concentrations around nearby sources. In this study, we use tropospheric NO_2 column observations made by the TROPOspheric Monitoring Instrument (TROPOMI) on the Sentinel-5 Precursor satellite over Nepal to characterize spatial and temporal variation with a focus over two highly polluted areas. NO_2 enhancement over the capital city of Kathmandu aligns with emissions from transportation and industrial sectors as observed in the bottom-up emission inventory. The highly resolved TROPOMI NO_2 observations reveal significant and growing NO_2

* Corresponding author.
** Corresponding author. NASA Goddard Space Flight Center, Greenbelt, MD, 20771, USA.
E-mail addresses: madhu.gyawali@sjcd.edu (M.S. Gyawali), lok.lamsal@nasa.gov (L.N. Lamsal).

https://doi.org/10.1016/j.aeaoa.2025.100324
Received 8 September 2024; Received in revised form 18 March 2025; Accepted 4 April 2025
Available online 9 April 2025

hotspots in rural and sparsely populated regions that align with the locations of various cement industries, brick kilns, and limestone mines. Most notably, the largest NO_2 concentration has been found above the Hongshi Shivam Cement industry and limestone mining areas. Our estimates of NO_x emissions for 2019–2021 using TROPOMI NO_2 observations and their comparison with bottom-up emissions from the EDGAR inventory for 2018 suggest comparable values over the Lumbini-Butwal-Palpa corridor but around 35 % higher estimates over Kathmandu.

1. Introduction

Over the last two decades, Nepal has been experiencing significant economic growth, domestic migration, urbanization, and industrialization (Ishtiaque et al., 2017; Rimal et al., 2018, 2020). With the excessive urbanization and the aftermath of the 2015 earthquake that damaged a quarter of a million buildings (Bothara et al., 2016), the demand for cement, bricks, and other construction materials has increased considerably. To meet these demands, there are currently ~1700 brick kilns producing ~5 billion units of bricks annually (Eil et al., 2020) and ~120 cement factories producing ~14 million metric tons of cement each year (Neupane et al., 2019). These phenomenal growths in the production of construction materials, combined with insufficient regulations typical of a developing country, exacerbate pollution levels in Nepal's major metropolitan cities (Bhattarai and Conway, 2021). The uncoordinated land use and land cover changes due to urbanization and a surge in the number of vehicles have led to a rise in air pollution levels, causing a range of health issues that has negatively impacted the nation's economy (Thapa et al., 2008). It is predicted that the demand for these construction materials could see a four-fold increase in the near future (Eil et al., 2020), which could further deteriorate air quality issues in the country.

Ambient air pollution is a leading risk factor, as more than 96 % of the global population in large cities are exposed to fine particulate matter ($PM_{2.5}$)levels which are above the warning level by the World Health Organization's (WHO) air quality standards (Krzyzanowski et al., 2014). While air quality impacts the global population, extreme air pollutant burdens are highest in cities in developing countries (Kumar et al., 2022). For instance, according to the United Nations Environment Programme (UNEP), the annual mean exposure of each individual in Nepal to fine particulate matter ($PM_{2.5}$) is 83 $\mu g/m^3$, which is about 16.6 times higher than the WHO set standard guideline value. This high level of exposure to particulate pollutants leads to an estimated 59 deaths per 100,000 people (UNEP, 2021). Despite the risks, air quality monitoring programs in many of the developing countries, including Nepal, are mostly limited to measuring particulate matter (Wei et al., 2022). Inadequate ground-based monitoring stations present challenges to measure $PM_{2.5}$ and suggest mitigation approaches of existing air pollution in the country (Gurung and Bell, 2012).

Nitrogen oxides (NO_x) are among the leading causes of deterioration of the ambient air quality, especially in urban and industrialized areas (Castellanos and Boersma, 2012). Nitrogen dioxide (NO_2) is a criteria pollutant, a precursor of ozone and nitrate aerosols, and an air quality indicator (Bernard et al., 2001; Hofzumahaus et al., 2009; Kumar et al., 2022; Li et al., 2019; Qu et al., 2021). The primary NO_x sources include combustion, soil emissions, and lightning (Fowler et al., 2013; Galloway et al., 2004; Schumann and Huntrieser, 2007; Wang et al., 2021). Near to the surface, NO_x is short-lived and has high concentrations near the source. Satellite instruments provide global observations of NO_2, allowing the detection of NO_x sources and quantification of their emissions and trends in developed and developing countries alike. High spatial resolution observations with improved signal-to-noise from the next generation instruments like TROPOspheric Monitoring Instrument (TROPOMI) has been playing a significant role in global air pollution monitoring.

Very few studies have been conducted on air quality studies in Nepal, with most research focusing on particulate matter and black carbon (Chelsea E. Stockwell et al., 2016; Weyant et al., 2014). The Nepal Ambient Monitoring and Source Testing Experiment (NAMaSTE) conducted a multiphase field campaign in 2015 April along the Indo-Nepal border in the Indo-Gangetic Plain (IGP), gathering data on PM and trace gases near to some specific sources. The findings identified brick and cement kilns as major contributors to particle pollutants (Jayarathne et al., 2018; C. E. Stockwell et al., 2016; Zhong et al., 2019). The Sustainable Atmosphere for the Kathmandu Valley – Atmospheric Brown Clouds (SusKat-ABC) project quantified the effects of pollution sources in the Kathmandu Valley (Mahata et al., 2018; Rupakheti et al., 2017). More recently, TROPOMI satellite data has been utilized to access the impact of COVID-19 lockdowns in NO_2 levels over major cities in Nepal (Dhital et al., 2022). Building on the prior studies, this study provides analysis of spatial and temporal variation of tropospheric NO_2 over Nepal, their emission sources, and detailed investigation of a new pollution hotspot that is growing at an alarming rate.

Although prior studies have recognized brick and cement kilns as a source of air pollution and can emit NO_x (Stockwell et al., 2016; Weyant et al., 2014), published reports on pollution from Nepal's brick and cement factories have mainly focused on pollutants like particulate matter and black carbon observed at limited surface sites (Weyant et al., 2014). Using tropospheric NO_2 column observations and analyzing spatial and temporal patterns, we demonstrate that TROPOMI can detect growing NO_2 levels over areas with highly concentrated cement and brick factories, and that these areas evolve as new pollution hotspots superseding highly polluted capital city of Kathmandu. The structure of the paper is as follows: In Section 2, we provide an overview of cement and brick factories as significant contributors of air pollution in Nepal. Section 3 provides a brief description of satellite observations, bottom-up emissions, and methods used. In Section 4, we present the results and discussion, and Section 5 concludes the study.

2. Contribution of Nepal's cement and brick industries on emissions

2.1. Cement industry

There are 114 registered cement industries in Nepal, but only 65 are currently operating by these produce ~14 million metric tons of cement annually (Neupane et al., 2019). Cement manufacturing in Nepal developed rapidly during 2004–2010 and has continued to grow since then. Cement production increased from 0.3 million metric tons per year until 2010 to 10 million metric tons in 2018. The demand for cement is driven by infrastructure projects such as construction of hydropower, road networks, and houses and commercial buildings, and demand especially increased during the post-earthquake reconstruction work in urban areas. This is also linked to the growth in gross domestic product (GDP) per capita in Nepal. Most cement industries are in the southern plains with ~$1/3^{rd}$ of the industries in the Lumbini-Butwal-Palpa corridor. Lumbini is one of the holiest places and a UNESCO heritage site. The Hongshi-Shivam Cement industry is the largest one in this corridor. It became operational in 2018 and can produce 6000 tons of cement per day. These cement industries are associated with 171 licensed limestone mining operations that produce raw materials in nearby hilly regions, which are then transported to work sites by hundreds of heavy trucks. Combustion of fuel used in these industries include the coal imported from South Africa and India. The thermal combustion of coal often exceeding 1400 °C in the kiln's burning zone are the major sources of NO_x emissions.

2.2. Brick factories

Nearly 1700 brick kilns operating in Nepal produce about 5 billion units of bricks per year (Eil et al., 2020). Brick factories are scattered in various parts of Nepal, but their concentrations are higher, mostly, in the

south-central and south-eastern regions. Most of these brick factories cease operation during the monsoon season (June–August) each year that often coincides with the crop harvesting/cultivating season. Brick kilns with permanently fixed chimneys are generally large and those with temporary chimneys are smaller and temporary in nature. Weyant et al. (2014) reported that coal is the primary input in most brick kilns, with 50 % of kilns using a combination of coal and rice husk, 26 % using a combination of coal, sawdust, and other biomass, and 24 % using coal as the only fuel. Combustion of these biomass and coal releases various gaseous (e.g., carbon monoxide, NO_x) and particle (e.g., black carbon) pollutants. Despite the widespread use of brick kilns in Nepal, the brick producing technology has remained largely unchanged for decades and is reported as highly inefficient, ineffectual, and polluting (Eil et al., 2020).

For this study, we gathered information about the location of these brick factories from various sources. Among these sources was Google Earth Pro that has updated locational information of all the brick factories with their names and addresses. Gathering these locations using Keyhole Markup Language (KML) and importing them into ArcGIS Pro as layer provides the exact location of each brick factory. These locations were later verified with the list of factories published by the Census Bureau of Statistics and the Ministry of Industry of the Government of Nepal.

3. Data and methods

3.1. Satellite NO_2 observations

3.1.1. TROPOMI

TROPOMI is a nadir-viewing satellite instrument launched on October 13, 2017 on board the Sentinel-5 Precursor satellite. The satellite flies at an altitude of 817 km in a near-polar sun-synchronous orbit with an equatorial overpass time in an ascending node at 13:30 local time with a repeat cycle of 17 days. With ground resolution as high as 3.5 × 5.5 km^2, TROPOMI can detect localized pollution plumes and identify small-scale emission sources such as industrial facilities and biomass burning emissions.

We obtained TROPOMI NO_2 data from the NASA Goddard Earth Sciences Data and Information Services Center (GES DISC, https://disc.gsfc.nasa.gov/datasets/TROPOMI_MINDS_NO2_1.1/summary). The NO_2 slant column retrievals are performed using ultraviolet–visible spectral data over the 405–465 nm range, as discussed in detail in (van Geffen et al., 2020) with the Version 2.3.1 updates (van Geffen et al., 2022). Conversion of slant to vertical column densities (VCD) and their separation into stratospheric and tropospheric components is done using the NASA NO_2 algorithm (Fisher et al., 2024; Lok N. Lamsal et al., 2021). We use tropospheric NO_2 column data with quality assurance (QA) values greater than 0.75, meaning that the scenes are mostly cloud-free, and grid them onto a regular size of 0.01° latitude × 0.01° longitude (~1.1 km × 1.1 km). The regridding method determines polygons intersecting a grid and calculates an average value for the grid, and is similar to the one used by the OMI Level 3 NO_2 product (Krotkov et al., 2019).

3.1.2. OMI

To study long-term NO_2 patterns (2005–2019), we also used data from the Ozone Monitoring Instrument (OMI) on NASA's Aura satellite. Launched in 2004, OMI provides daily coverage, with measurements of solar and backscatter radiation in the ultraviolet–visible spectral range (264 nm–504 nm) with a resolution of ~0.6 nm (Boersma et al., 2007, 2008; Lamsal et al., 2015, 2021). Here, we used the OMI NO_2 Standard Product version 4.0, available from NASA's Goddard Earth Sciences Data Active Archive Center (Lamsal et al., 2021). This product, based on the differential optical absorption spectroscopy (DOAS) technique, includes significant improvements in the air mass factor calculation, enhancing its accuracy (Lamsal et al., 2021). We used gridded tropospheric NO_2 column data at 0.1° latitude x 0.1° longitude resolution that are created using high-quality data with an effective cloud fraction below 0.3, excluding data affected by row anomalies (Dobber et al., 2008).

3.2. EDGAR bottom-up emission inventory

We compute total NO_x emissions using the data from various sectors from the Emission Database for Global Atmospheric Research (EDGAR) emission inventory, v6.0, for the year 2018 (https://edgar.jrc.ec.europa.eu/emissions_data_and_maps). This inventory, available at 0.1° latitude × 0.1° longitude, covers 26 aggregated sources and 64 fuel types, and utilizes splitting factors derived from the Energy Information Administration data on coal, oil, and natural gas fuel consumption (Crippa et al., 2018). The emissions for a particular country are determined based on the technologies employed, as well as the dependency of emission factors on fuel type, combustion conditions, and activity data. Our use of these data here is limited to providing contributions of various emission sources and examining their consistency with TROPOMI NO_2 observations.

Fig. 1 shows annual total NO_x emissions for 2018 in Nepal separated by source types and regional contributions. Transportation, manufacturing, energy for building, and agriculture are major emission sources contributing 96 % of total emissions in Nepal. Close to 1% contribution comes from miscellaneous sources consisting of small industries such as food processing, paper, manure management, oil refineries, and solid waste incineration. These industries contribute ~48 % emissions in the Terai region, 45 % in the mid-hills, and 7 % in the Himalayan regions. The Kathmandu Valley contributes 10 % and Lumbini-Butwal-Palpa corridor contributes 3.7 % of the total NO_x emission.

3.3. The directional derivative approach for top-down NO_x emission estimates

We employ the directional derivative approach to estimate NO_x emissions from TROPOMI for 2019–2021. This technique, previously utilized by Lonsdale and Sun (2023, 2022) to derive NO_x emissions from satellite-observed column amounts, is based on the principle of mass conservation. Details on the method, assumptions, and limitations are thoroughly discussed in these references (Lonsdale and Sun, 2023; Sun, 2022). Briefly, the directional derivative approach estimates NO_x emissions by integrating multiple factors influencing the distribution

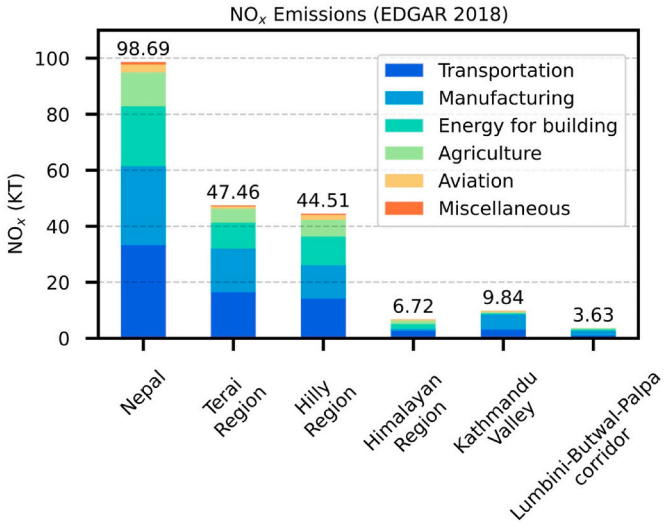

Fig. 1. EDGAR NO_x emissions for 2018 segregated by source types and geographic regions over Nepal.

and concentration of NO_2. The wind-gradient and wind-topography terms are derived from the directional derivatives of TROPOMI tropospheric NO_2 column observations discussed in Section 3.1.1 and surface altitude with respect to the horizontal winds near the surface. Coincidently sampled wind data are taken from the European Centre for Medium-Range Weather Forecasts (ECMWF). The scale height and vertically integrated chemical lifetime are calculated from linear regression coefficients. We use high quality data with quality assurance value exceeding 0.75, apply the physical oversampling approach as described in (Sun et al., 2018) to create data at ~1 km resolution, perform emission calculations at that resolution, and aggregate them over 0.1° latitude x 0.1° longitude grids of the EDGAR emission inventory discussed above.

The directional derivative provides valuable insights into emission patterns and their temporal variations by considering various influencing factors. However, the approach has limitations, including reliance on the principle of mass conservation and the accuracy of input data, which can introduce inaccuracies due to assumptions and simplifications. Additionally, using linear regression coefficients to estimate chemical lifetime and scale height may not fully capture the complex and nonlinear nature of atmospheric chemistry. Spatiotemporal averaging can smooth out significant variations, potentially masking important emission events or trends. Variations in planetary boundary layer dynamics and inherent uncertainties in satellite observations can impact the accuracy of the inferred emissions.

4. Results and discussion

4.1. Sources and NO_2 variations across Nepal

Fig. 2a and b shows 3-year (2019–2021) average TROPOMI tropospheric NO_2 columns and EDGAR NO_x emissions for 2018, respectively. The spatial distribution of NO_2 over Nepal is characterized by a clear north-south gradient with higher values in the southern part bordering with India and lower values in the northern mountainous regions, reflecting consistency with the distribution of brick and cement industries shown in 2c and population density shown in 2d. A significant hotspot is evident over the Kathmandu valley, reflecting higher NO_x emissions as observed in the EDGAR emission inventory. In addition to typical emission sources (e.g., transport, industries), an estimated 122 brick kilns are operating around the valley. Notable NO_2 enhancement is also observed in the encircled Lumbini-Butwal-Palpa corridor in the southern part of the country that corresponds to high concentration of brick and cement industries. This area consists of 90 brick kilns and 24 cement industries that include Hongshi Shivam Cement. The lack of similar enhancement in NO_x emissions and the inconsistency between TROPOMI observations and EDGAR NO_x emissions may suggest that these emission sources could be either missing or not well-represented in the emission inventory.

Fig. 3 shows the land use and land cover map of Nepal (Fig. 3a) in 2020 with zoomed map for the Kathmandu Valley (Fig. 3b), and the Lumbini-Butwal-Palpa corridor (Fig. 3c), the two NO_2 hotspots observed by TROPOMI. A massive expansion of urban built-up areas in the Kathmandu Valley (Fig. 3b) and an expansion of agricultural land in the

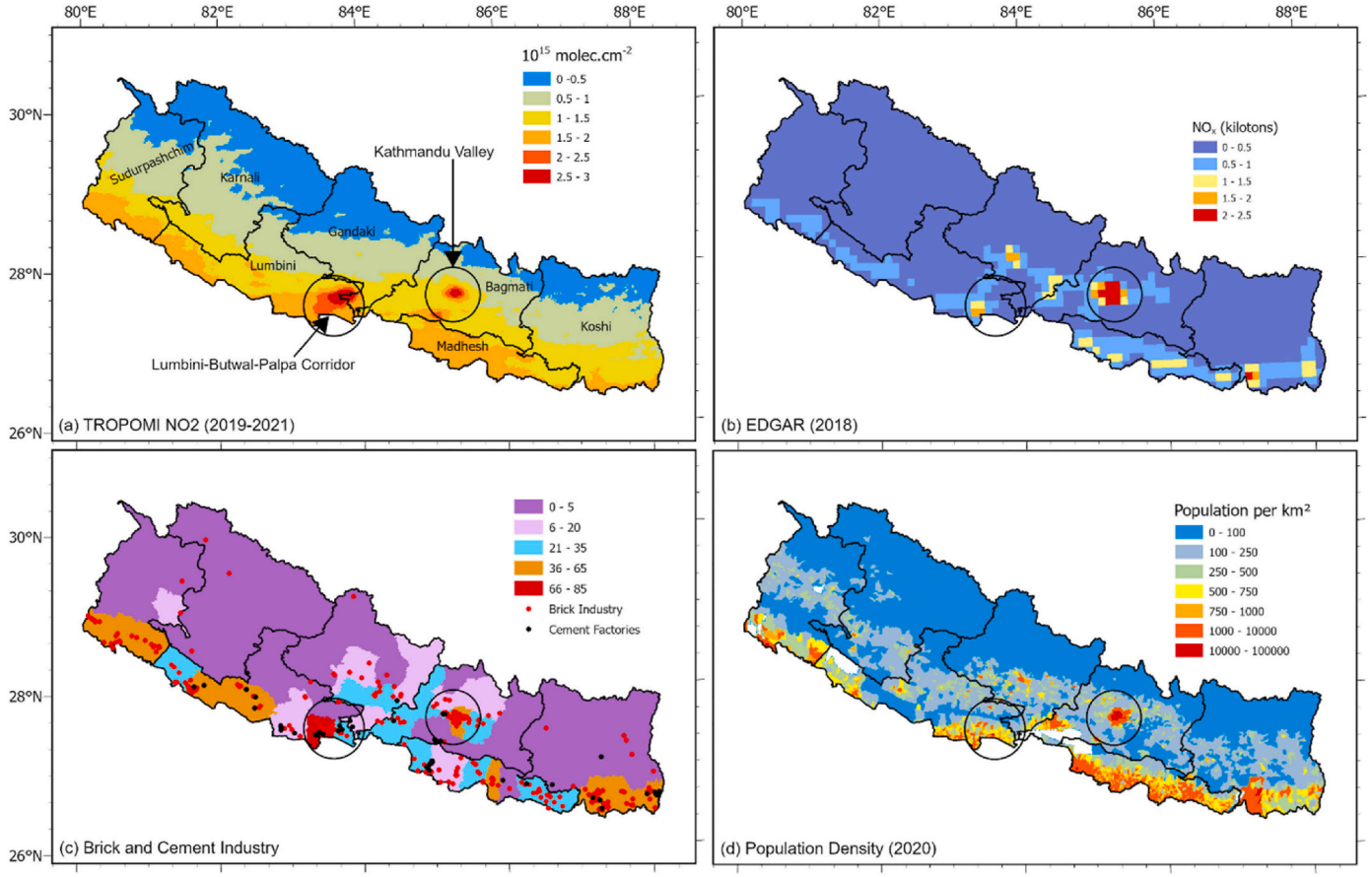

Fig. 2. Maps of Nepal showing the (a) average TROPOMI tropospheric NO_2 columns for the period 2019–2021, and (b) NO_x emission estimates for 2018 calculated using Emission Database for Global Atmospheric Research (EDGAR), (c) location and distribution of brick (red circles and colored districts) and cement (black circles) industries, (d) population density for 2020. Circled areas indicate Kathmandu Valley and Lumbini-Butwal-Palpa corridor. The pink lines show provincial boundaries. (For interpretation of the references to color in this figure legend, the reader is referred to the Web version of this article.)

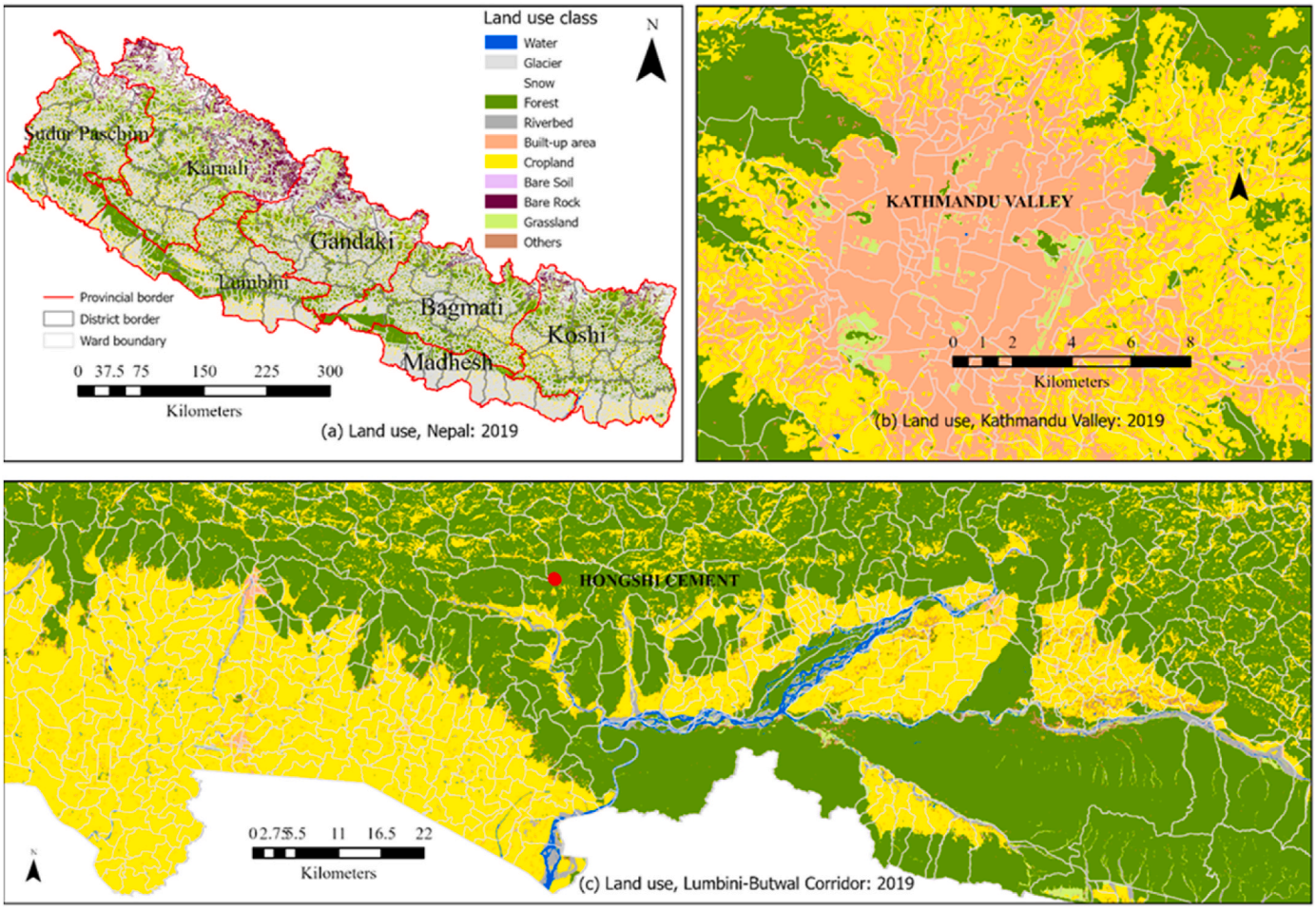

Fig. 3. Land use and land cover situation of Nepal (Fig. a), the Kathmandu Valley (Fig. b), and Lumbini-Butwal-Palpa corridor (Fig. c). The red circled area indicates the location of the Hongshi-Shivam cement factory. (For interpretation of the references to color in this figure legend, the reader is referred to the Web version of this article.)

Lumbini-Butwal-Palpa corridor (Fig. 3c) are evident. The capital city is a bowl-shaped area with dense urban structure and built-up areas that experiences heavy pollution typical of many Asian cities which is reflected in enhanced TROPOMI NO_2 column observations. Contrary to this is the Lumbini-Butwal-Palpa corridor with mostly cropland and forest areas and without any urban built-up, suggesting that the NO_2 enhancement over this region is largely from cement and brick industries that are predominantly located in the region.

Fig. 4 shows seasonal tropospheric NO_2 columns maps from TROPOMI over a region featuring the two most highly polluted areas in the country. A clear seasonality exists with a maximum in winter and minimum in summer, reflecting changes in NO_x lifetime. We attribute the relatively low NO_2 levels during the summer season to a combined effect of 1) reduced NO_x lifetime in summer, 2) significant reduction in brick and cement production during the monsoon period, and 3) enhanced effect of wet deposition during the rainy seasons. The sustained and uniformly elevated NO_2 levels observed beyond these source regions during spring are due to NO_x emissions from agricultural burning practices in Nepal and northern India. It is worthwhile noting that the NO_2 levels in the Butwal-Palpa corridor significantly surpass those in Kathmandu Valley in all seasons.

4.2. Enhanced NO_2 pollution from cement and brick factories

Fig. 5 shows a zoomed map of average TROPOMI NO_2 columns for winter months of 2019–2021 over the Lumbini-Butwal-Palpa corridor. As discussed above in Sections 2 and 4.1, this area has experienced significant growth as a major center for cement manufacturing alongside the well-established brick industry. The Department of Industry reports that there are about 40 cement factories in the area which contribute ~40 % of the country's total cement production. The significant NO_2 enhancement observed in Fig. 5 is due to contributions from several factors. First, the Hongshi-Shivam Cement Industry with its limestone mine spanning~ 10 km radius is located near the hotspot (Fig. 3c). This is the largest cement factory in Nepal producing 6000 tons of both cement and clinker daily, while its optimum production capacity is twice as large. Cement manufacturing, in general, is an energy intensive process with coal as the main energy source and a significant emission source. Second, before connected to the national transmission line in November 2021, this cement industry was generating electricity via its fourteen 1.4 MW diesel generators that consumed 60,000 L of diesel each day. Third, extraction of limestone from several large quarries for Hongshi-Shivam and other cement industries occur along the north hilly regions located in the neighboring Palpa and Arghakanchi districts (Fig. 5). Third, hundreds of heavy trucks and other machinery equipment that operate on a regular basis contribute to the enhanced NO_2 columns. Finally, the general enhancement over large areas is due to the impact of nearby brick and smaller cement industries as well as the plumes advected by the prevailing winds.

Fig. 6a demonstrates how NO_2 pollution in the semi-rural, non-urban area of the Lumbini-Butwal-Palpa corridor with a high number of cement and brick factories is rapidly outpacing highly urbanized capital city of Kathmandu. Shown in the figure are monthly time series of average TROPOMI tropospheric NO_2 VCD over a 0.3° x 0.3° grid from

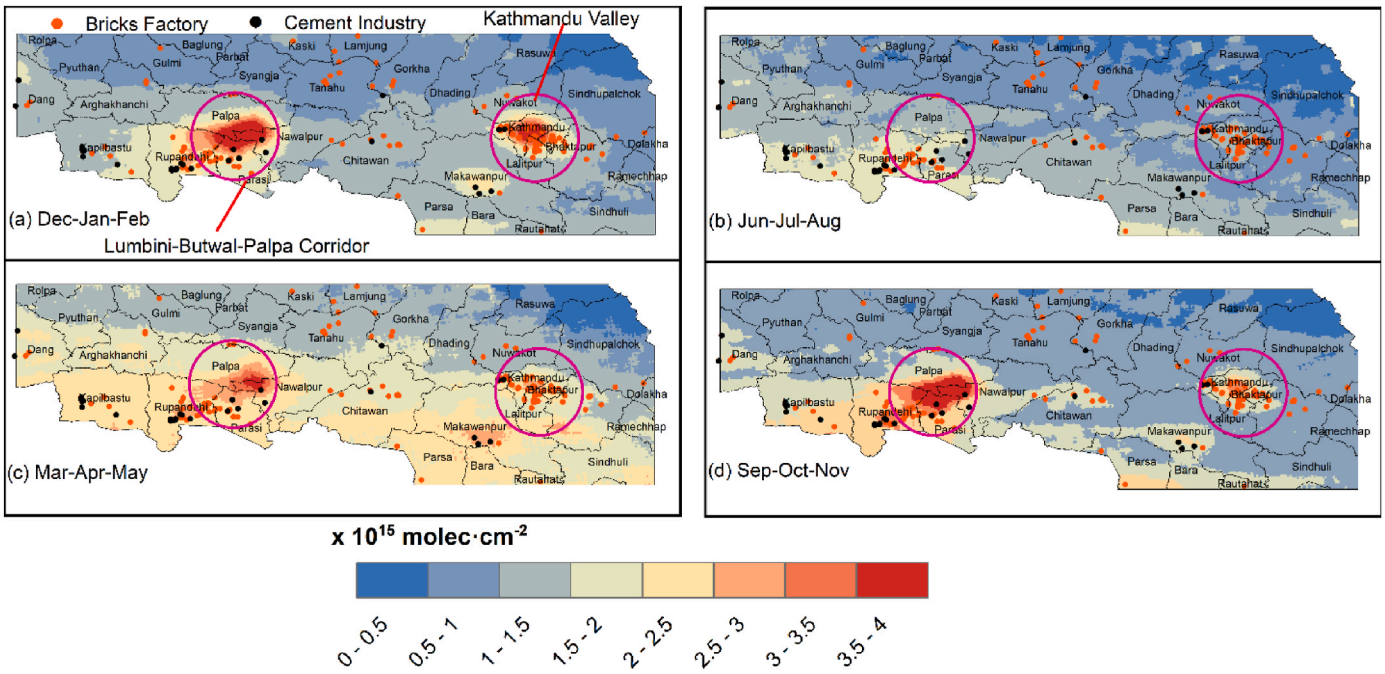

Fig. 4. The seasonal average tropospheric NO_2 VCD for winter (December–February), spring (March–May), summer (June–August) and fall (September–November) from TROPOMI. Spatial resolution of the data is 0.01° latitude x 0.01° longitude. The images are zoomed over the hotspot regions in Kathmandu and near Lumbini. The map also displays the distribution of cement and brick industries.

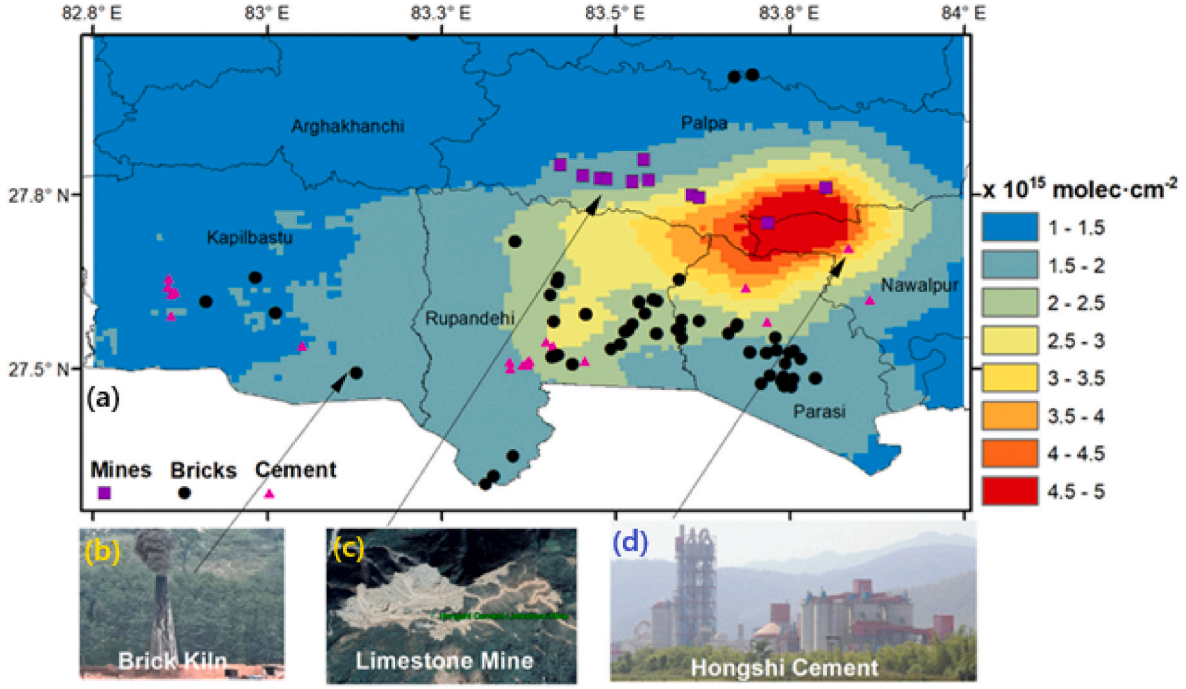

Fig. 5. A zoomed map of three year (2019–2021) average tropospheric NO_2 columns in winter (December-January-February) from TROPOMI over a ~64 km by 36 km area around the Lumbini-Butwal-Palpa corridor in southern Nepal. Location of major emission sources are indicated for cement industries (pink triangles), brick kilns (black circles), and limestone mining areas (purple squares). The major hotspot is located close to the newly built Hongshi Shivam Cement Industry. (For interpretation of the references to color in this figure legend, the reader is referred to the Web version of this article.)

the two encircled areas in Fig. 4. As discussed earlier, NO_2 variation exhibits a clear seasonality in both areas with a maximum in winter and a minimum in summer. A notable difference is evident in annual changes with considerable year to year increase over Lumbini-Butwal-Palpa corridor but nearly a steady scenario over Kathmandu valley. Over the Lumbini-Butwal-Palpa corridor region NO_2 nearly doubles in three years. This change is rather dramatic considering the ~3.5%/year change in tropospheric NO_2 columns observed over both regions by OMI since 2005 as discussed further in Section 3.5. While studies on NO_2 emissions from cement and brick industries are scarce, our findings are consistent with Dhital et al. (2022), which reported a decline in NO_2 levels over Kathmandu during the COVID-19 lockdown using TROPOMI

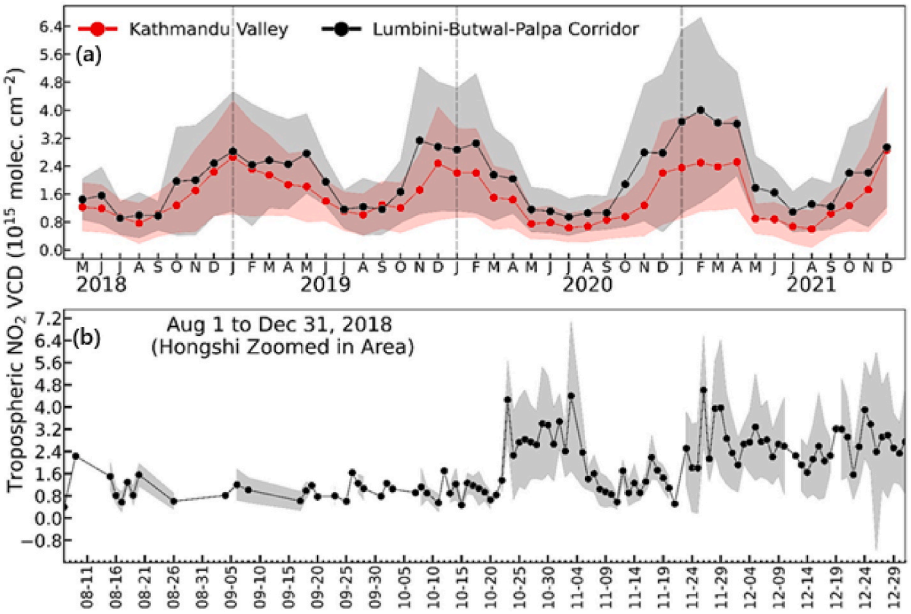

Fig. 6. (a) A time series of the average monthly TROPOMI tropospheric NO_2 columns over a 0.3° x 0.3° grid over Lumbini-Butwal-Palpa corridor (black) and Kathmandu Valley (red). The shaded areas represent the monthly variability (standard deviation). (b) A daily average (black line) and standard deviation (gray shade) over a circular domain around the Hongshi-Shivam Cement during August 1st to December 31st of 2018, when the cement industry started the operation. (For interpretation of the references to color in this figure legend, the reader is referred to the Web version of this article.)

data. However, their study focused on short-term changes, whereas our analysis from 2018 to 2021 shows a continuous rise in NO_2 over the Lumbini-Butwal-Palpa corridor, largely due to the expansion of cement and brick industries.

Fig. 6b presents a daily time series showing average tropospheric NO_2 columns within a circular area encompassing the Hongshi-Shivam cement industry. Up until October 20, 2018, NO_2 columns were relatively stable and low, with values hovering around 1.0×10^{15} molec. cm^{-2}. A sudden and notable three- to four-fold surge in NO_2 levels occurred in late October and early November. Information on the exact start date for the operation of the newly built Hongshi-Shivam cement factory was not available, but TROPOMI NO_2 observations suggest that the enhancement could be related to the initial operational and testing phase. There are no other emission sources in this remote area with limited population and development. Substantial power generation with more than a dozen diesel generators combined with the use of coal for cement production could result in the high emission levels detected by TROPOMI. This demonstration serves as an example of the power of satellite observations to monitor pollution for areas that do not have ground monitoring stations, such as remote and inaccessible regions, with their ability to provide near global coverage.

4.3. NO_x emission estimates over the two subregions

We used the directional derivative method (described in section 2.3) to quantify NO_x emissions over the Lumbini-Butwal-Palpa corridor and Kathmandu valley. Fig. 7 shows estimated NO_x emissions for the year 2019, 2020, and 2021. The NO_x emissions exhibit spatial patterns similar to those of tropospheric NO_2 columns with elevated emissions over Kathmandu and the Lumnini-Butwal-Palpa corridor. The remaining areas reveal negligible emissions, indicating minimal human activity and the absence of major industries. Additionally, the largely forested land (as depicted in Fig. 3) showed almost no emissions. The maps reveal the consistent annual increase in NO_x emissions over the Butwal-Palpa

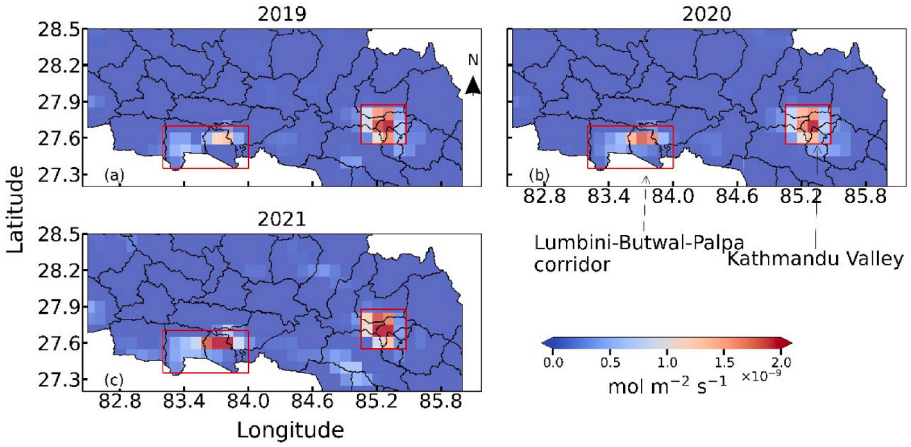

Fig. 7. Annual NO_x emissions derived using the direction derivative approach for (a) 2019, (b) 2020, and (c) 2021. Bounding boxes in red over Kathmandu Valley and Lumbini-Butwal-Palpa corridor are used for estimating NO_x emissions in Table 1. (For interpretation of the references to color in this figure legend, the reader is referred to the Web version of this article.)

corridor. This suggests rapid changes in the Butwal-Palpa corridor due to the expansion of brick and cement industries. A slight decrease in emissions over Kathmandu Valley in 2020 reflects the impact of COVID-19 due to reduced transportation and industrial activities.

Table 1 lists the total annual NO_x emissions for two selected domains in the Lumbini-Butwal-Palpa corridor and Kathmandu Valley. NO_x emissions derived using TROPOMI observations over Kathmandu Valley are nearly stable and consistent across all three years with annual total emissions close to 6 kT/year. A slight decrease in 2020 over the capital city, which is traditionally the most polluted region in the country with the highest population and largest number of daily active vehicles in the country, could be COVID-19-related. In contrast, the annual increase in emissions over the Lumbini-Butwal-Palpa corridor is 36% in 2020 and 41% in 2021. Most of the increase occurs over a small region near Hongshi-Shivam Cement and other cement industries. The total NO_x emissions in this region is on par with the number of emissions in Kathmandu Valley.

Comparison of 2018 EDGAR NO_x emissions with NO_x emissions derived using TROPOMI observations suggests that the emissions in EDGAR are comparable over the Lumbini-Butwal-Palpa corridor, but roughly 35% higher than the capital city (Table 1). Rapid changes in emissions over the Lumbini-Butwal-Palpa corridor increase the discrepancies with EDGAR emissions being higher by 12% in 2019 and lower by 68% in 2021. The observed discrepancies over these two regions suggest the possibilities of: 1) larger uncertainty in emission factors in the development of bottom-up emission inventory and a need to update activity data and emission factors; 2) larger uncertainty in satellite retrievals over the complex terrain of Nepal; and 3) various limitations inherent in the directional derivative method. The emissions derived from the directional derivative method may be affected by simplified assumptions on NO_x lifetime, NO to NO_2 ratio, species' scale height, etc., that may not hold true in all cases, potentially resulting in inaccurate emission estimates (Lonsdale and Sun, 2023). Moreover, the quality of satellite retrievals can degrade over complex terrain in Nepal due to larger uncertainty in a-priori NO_2 profile shape, terrain pressure, surface reflectivity, and lack of explicit aerosol correction in the retrieval process (Lamsal et al., 2021). Details on satellite retrieval uncertainties can be found in previous studies (Boersma et al., 2011; Lamsal et al., 2021).

4.4. Long-term perspective from OMI NO_2 observations

For a long-term perspective, we analyze multi-year (2005–2019) datasets of tropospheric NO_2 columns from OMI that provides extensive spatial coverage and consistent data, albeit with a coarser ground resolution as compared to TROPOMI. We conduct trend analysis by employing the multivariate linear regression method discussed in detail in Lamsal et al. (2015) and was also utilized in Duncan et al. (2016) and Gyawali et al. (2023). This method separates short and long-term variation in the monthly average data into three key components: a linear trend term representing long-term NO_2 changes, a time-dependent seasonal component that characterizes variations over the months since January 2005, and a residual or noise component. Absolute changes in OMI NO_2 are then computed by employing two least-squares regression models on the de-seasonalized time series. The estimated trend was deemed statistically significant at a 95 % confidence level.

Table 1
Total annual NO_x emission estimates from TROPOMI and EDGAR over selected domains in Kathmandu Valley and Lumbini-Butwal-Palpa corridor shown in Fig. 7.

Domain/Data source	TROPOMI (KT)			EDGAR (KT)
	2019	2020	2021	2018
Kathmandu Valley	6.30	5.83	6.44	9.84
Lumbini-Butwal-Palpa corridor	3.17	4.32	6.09	3.63

Fig. 8 shows spatial variation in tropospheric NO_2 trend over Nepal during 2005–2019 as observed by OMI. Statistically significant positive trends reaching up to 80 % are observed over large part of the country, especially in the southern part bordering with India. The most significant changes are observed in areas with high NO_2 levels, particularly over Kathmandu and Lumbini-Butwal-Palpa corridor. Sparsely inhabited hilly areas in the central part and mountainous areas in the north with no significant emission sources lack any clear trend.

Fig. 9 shows monthly tropospheric NO_2 columns over an area of size 0.5° latitude × 0.5° longitude in Kathmandu Valley. Since background and seasonal patterns dominate a large part of NO_2 variation, we separate those components from OMI NO_2 data and calculate de-seasonalized NO_2 values shown in the lower panel. Isolation of long-term changes and transient, short-term fluctuations emanating from weather and other events allows us to calculate annual NO_2 trend and its uncertainty over the domain. We observe a gradual increase in NO_2 levels since 2005 with an annual increase of 3.5 ± 0.8 % over Kathmandu and 3.6 ± 1.3 % over Lumbini-Butwal-Palpa corridor.

4.5. Socioeconomic and environmental implications of brick and cement industries

The cement and brick industries are essential for Nepal's developing economies because the country is going through many infrastructure projects in association with significant urbanization. For example, in 2015, Nepal's urban classified population reached 66% from 23% in 2014 (Bhattarai et al., 2023). Added to that, the mega earthquakes of 7.8 Richter Scale on April 25, 2015, rattled many infrastructures of Nepal needing their reconstruction. The consumption of cement has been increasing in Nepal after 2015 with an increase in annual demand from 4.5 million tons in 2014–2015 to 9.1 million tons in 2018–2019 and 25.9 million tons in 2025 (Nepal Rastra, 2021). Likewise, following the 2015 earthquake the country's annual brick production has increased from 5 billion to 12 billion bricks annually (Bajracharya et al., 2021). Although most of the reconstruction activities could have been completed, the demand for cement and bricks is unlikely to subside for three main reasons. First, Nepal aims to progress from one of the less-developed economies to developing economic status earliest by 2024, at the latest by 2026. Second, it plans to achieve sustainable development goals (SDG) by 2030. Third, the National Planning Commission of Nepal has identified 22 national pride projects. All these activities will increase the demand for cement and bricks within the country, and the government intends to boost the domestic cement production capacity. These industries require a considerable number of raw materials extracted locally (e.g., limestone ore and clay) and imported from other nations (e.g., coal, diesels) that have a wide range of implications. In particular, the environmental impact from these industries is colossal. Fossil fuel combustion in cement and brick productions emit various gases (e.g., carbon dioxide, NO_2, sulfur dioxide) and particulate (e.g., $PM_{2.5}$) pollutants. Inhalation of some of these pollutants can lead to respiratory problems and other health issues (Bhattarai et al., 2024; Kim et al., 2020). Processing raw materials such as limestone and clay results in various forms of environmental pollution (dust, gas emissions, sound) that directly impact local communities, contribute to soil erosion and sedimentation, and disrupt neighboring ecosystems and biodiversity. For instance, there are reports of several environmental and social problems at the historic site of Lumbini (BBC News, 2017) from air pollution. Noise and dust pollution caused by limestone carrying trucks passing through multiple schools is of concern for the well-being of school children in the region (Kathmandu Post, 2022). These societal and environmental issues could be addressed by adopting cleaner production technologies & practices and assessing gaseous & dust emissions through a routine monitoring of air quality. Satellite observations, as demonstrated in this study, could provide a valuable resource for air pollution monitoring in areas where ground monitors are sparse or nonexistent.

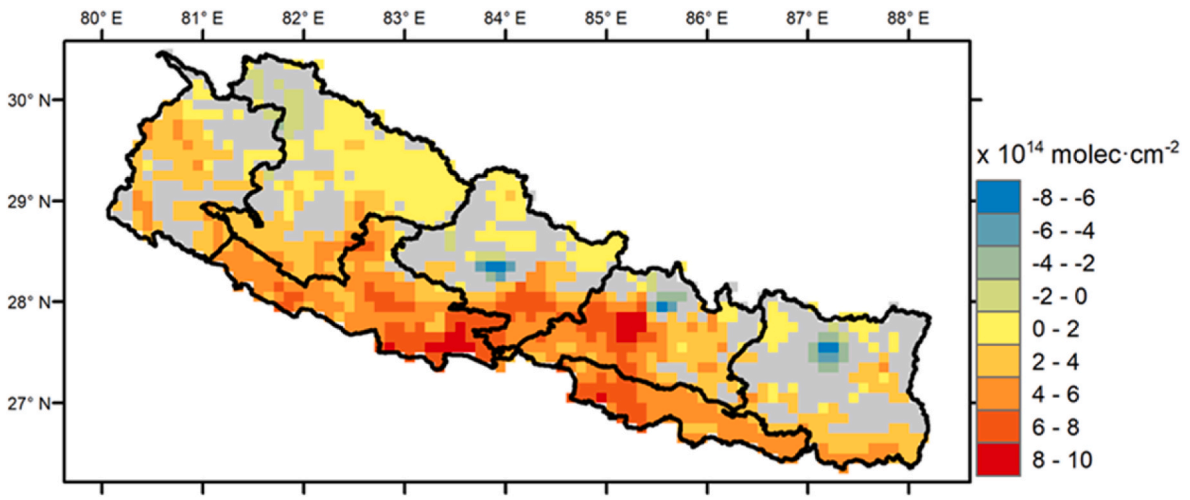

Fig. 8. Long-term changes in OMI tropospheric NO_2 columns from 2005 to 2019 over Nepal as derived from the linear trend. Colored areas represent a statistically significant trend at 95 % confidence. Gray areas represent where there are not statistically significant changes. The spatial resolution of the data is 0.1° latitude × 0.1° longitude.

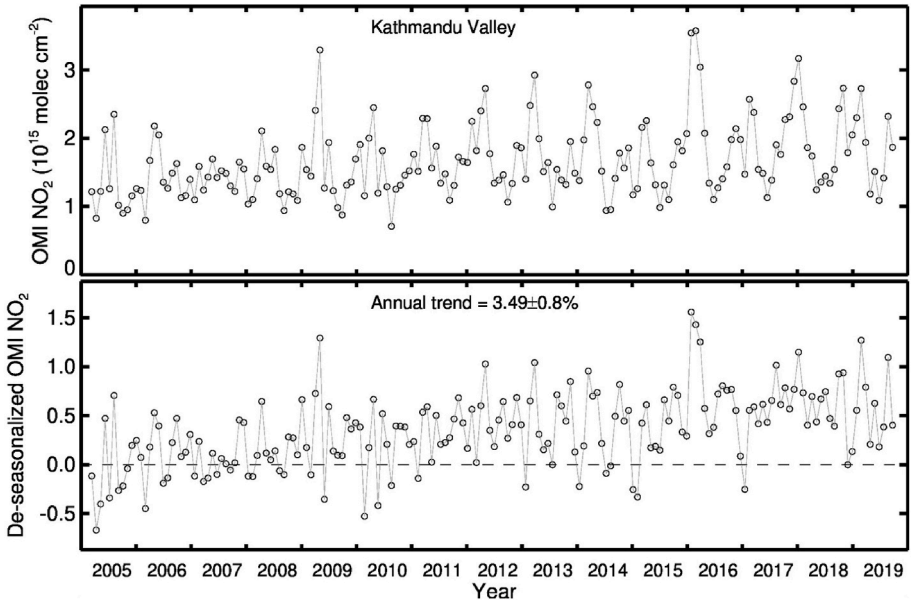

Fig. 9. Changes in OMI NO_2 tropospheric columns from 2005 to 2019 over Kathmandu, Nepal (top) Time series of monthly average OMI tropospheric NO_2 column data and (bottom) their de-seasonalized values averaged over a box of size 0.5° × 0.5° over Kathmandu. The dotted line in the bottom figure represents the 2005 baseline. The annual trend and its uncertainty are indicated.

5. Conclusions

In this study, we analyzed satellite tropospheric NO_2 column observations over Nepal by conducting a detailed analysis over two major source regions: Kathmandu Valley and the Lumbini-Butwal-Palpa corridor in southern Nepal. TROPOMI observations show a characteristic seasonal variation of NO_2 with higher values in winter and lower values in summer, reflecting seasonal changes in NO_x lifetime and enhanced deposition during the monsoon season. The springtime enhancements are due to biomass burning in the region. The spatial pattern of NO_2 is consistent with population data and emission patterns, with higher NO_2 levels in the heavily populated southern areas and lower levels in the sparsely populated mountainous regions in the north. An expected hotspot that agrees with bottom-up emission estimates over Kathmandu Valley reflects large-scale vehicle use and industrial activities. An additional hotspot contrasting with the emission inventory can be seen in the Lumbini-Butwal-Palpa corridor; the NO_2 pollution hotspot is geographically correlated with the locations of cement and brick industries that have grown substantially after the 2015 earthquake. This region with a high concentration of cement and brick industries, including the recently built Hongshi-Shivam cement industry, has evolved as a significant NO_2 pollution hotspot, surpassing the capital city of Kathmandu. TROPOMI observations over the region suggest nearly a twofold increase in NO_2 levels between 2019 and 2021, far exceeding the long-term historical growth rate of ~3.5 % per year observed by the Ozone Monitoring Instrument since 2005.

Using tropospheric NO_2 column observations from TROPOMI and coincidentally sampled wind data from ECMWF and by applying the directional derivative approach, we inferred top-down NO_x emissions for the years 2019–2021 over the two major source regions. The inferred top-down annual total NO_x emissions over Kathmandu Valley vary between 5.8 KT in 2020 and 6.4 KT in 2021 that are 34–40% lower than

the 9.8 KT emissions in 2018 calculated from the EDGAR inventory. Over the Lumbini-Butwal-Palpa corridor, the top-down emissions in 2019 and bottom-up emissions in 2018 are comparable, but the discrepancies increase for later years reaching nearly twofold in 2021. These discrepancies over the capital city and the regions experiencing a large-scale development of cement and brick industries underscore the need for timely updates in the bottom-up emission inventory.

This research has highlighted the importance of high-resolution satellite observations for identifying pollution from individual sources (Filonchyk and Peterson, 2023), which is particularly critical for detecting smaller sources, such as cement and brick factories, as analyzed in this study. Local measurements from ground-based monitors would provide real-time data for air quality assessment, source identification, and emission reduction support. Such measurements would also be helpful in validating satellite data, ensuring the reliability and accuracy of satellite products. Improved satellite retrievals and top-down inversion approaches are crucial for accurate NO_x emission estimates. Recent advances in geostationary air quality observations, such as Geostationary Environment Monitoring Spectrometer (GEMS (Kim et al., 2020),) over Asia and Tropospheric Emissions: Monitoring of Pollution (TEMPO (Zoogman et al., 2017),) over North America, will revolutionize air quality monitoring through hourly, high-resolution measurements.

CRediT authorship contribution statement

Madhu S. Gyawali: Writing – review & editing, Writing – original draft, Validation, Supervision, Methodology, Formal analysis, Data curation, Conceptualization. **Lok N. Lamsal:** Writing – review & editing, Writing – original draft, Methodology, Formal analysis, Conceptualization. **Sujan Neupane:** Writing – review & editing, Writing – original draft, Visualization, Formal analysis. **Bimal Gyawali:** Writing – review & editing, Writing – original draft, Visualization, Formal analysis. **Keshav Bhattarai:** Writing – review & editing, Writing – original draft, Visualization, Conceptualization. **Bradford Fisher:** Writing – review & editing, Writing – original draft, Formal analysis. **Nickolay Krotkov:** Writing – review & editing, Writing – original draft, Conceptualization. **Jos van Geffen:** Writing – review & editing, Writing – original draft, Conceptualization. **Henk Eskes:** Writing – review & editing, Writing – original draft, Conceptualization. **Shriram Sharma:** Writing – review & editing, Writing – original draft, Conceptualization. **Cameron Brunt:** Writing – review & editing, Writing – original draft, Formal analysis. **Rudra Aryal:** Writing – review & editing, Writing – original draft, Conceptualization.

Data availability statement

TROPOMI NO_2 data are freely available and downloaded from the NASA Goddard Earth Sciences Data and Information Services Center (GES DISC, https://disc.gsfc.nasa.gov/datasets/TROPOMI_MINDS_NO2_1.1/summary). OMI NO_2 data used here are available from the NASA Aura Validation Data Center website (https://avdc.gsfc.nasa.gov/pub/data/satellite/Aura/OMI/V03/L3/).

Declaration of competing interest

The authors declare no competing interests that could have influenced the interpretation of this work.

Acknowledgements

We would like to thank San Jacinto College, Texas, for facilitating this research and promoting collaboration with various agencies and Universities. We also thank Franklin Pierce University, Rindge, NH, for supporting co-author Rudra Aryal's research collaboration and contribution to the publication of this work. We acknowledge the free publicly available TROPOMI NO_2 data from the NASA Goddard Earth Sciences Data and Information Services Center (GES DISC, https://disc.gsfc.nasa.gov/datasets/TROPOMI_MINDS_NO2_1.1/summary and OMI NO2 data from the NASA Aura Validation Data Center website (https://avdc.gsfc.nasa.gov/pub/data/satellite/Aura/OMI/V03/L3/).

References

Bajracharya, S.B., Gurung, K., Mathema, L., Sharma, S., Mishra, A., 2021. Forgotten contributors in the brick sector in Nepal. Int. J. Environ. Res. Publ. Health 18, 6479. https://doi.org/10.3390/ijerph18126479.

BBC News, 2017. Buddha's birthplace faces serious air pollution threat. BBC News [WWW Document]. https://www.bbc.com/news/science-environment-39772099. accessed 2.2.24.

Bernard, S.M., Samet, J.M., Grambsch, A., Ebi, K.L., Romieu, I., 2001. The potential impacts of climate variability and change on air pollution-related health effects in the United States. Environ. Health Perspect. 109, 199–209. https://doi.org/10.1289/ehp.109-1240667.

Bhattarai, K., Adhikari, A.P., Gautam, S.P., 2023. State of urbanization in Nepal: the official definition and reality. Environ Challenges 13, 100776. https://doi.org/10.1016/j.envc.2023.100776.

Bhattarai, K., Conway, D., 2021. Contemporary Environmental Problems in Nepal: Geographic Perspectives, Advances in Asian Human-Environmental Research. Springer International Publishing, Cham. https://doi.org/10.1007/978-3-030-50168-6.

Bhattarai, K., Lamsal, L., Gyawali, M., Neupane, S., Gautam, S.P., Bakshi, A., Yeager, J., 2024. Impact of nitrogen dioxide (NO2) pollution on asthma: the case of Louisiana state (2005–2020). Atmosphere 15, 1472. https://doi.org/10.3390/atmos15121472.

Boersma, K.F., Eskes, H.J., Dirksen, R.J., van der A, R.J., Veefkind, J.P., Stammes, P., Huijnen, V., Kleipool, Q.L., Sneep, M., Claas, J., Leitão, J., Richter, A., Zhou, Y., Brunner, D., 2011. An improved tropospheric NO_2 column retrieval algorithm for the Ozone Monitoring Instrument. Atmos. Meas. Tech. 4, 1905–1928. https://doi.org/10.5194/amt-4-1905-2011.

Boersma, K.F., Eskes, H.J., Veefkind, J.P., Brinksma, E.J., Levelt, P.F., Stammes, P., Gleason, J.F., Bucsela, E.J., 2007. Near-real time retrieval of tropospheric NO2 from OMI. Atmos. Chem. Phys. 16.

Boersma, K.F., Jacob, D.J., Bucsela, E.J., Perring, A.E., Dirksen, R., van der A, R.J., Yantosca, R.M., Park, R.J., Wenig, M.O., Bertram, T.H., Cohen, R.C., 2008. Validation of OMI tropospheric NO2 observations during INTEX-B and application to constrain NOx emissions over the eastern United States and Mexico. Atmos. Environ. 42, 4480–4497. https://doi.org/10.1016/j.atmosenv.2008.02.004.

Bothara, J., Ingham, J., Dhakal, R., Dizhur, D., 2016. The Challenges of Housing Reconstruction after the April 2015 Gorkha, Nepal Earthquake. Nepal Engineers' Association - Technical Journal XLIII, pp. 121–134.

Castellanos, P., Boersma, K.F., 2012. Reductions in nitrogen oxides over Europe driven by environmental policy and economic recession. Sci. Rep. 2, 265. https://doi.org/10.1038/srep00265.

Crippa, M., Guizzardi, D., Muntean, M., Schaaf, E., Dentener, F., van Aardenne, J.A., Monni, S., Doering, U., Olivier, J.G.J., Pagliari, V., Janssens-Maenhout, G., 2018. Gridded emissions of air pollutants for the period 1970–2012 within EDGAR v4.3.2. Earth Syst. Sci. Data 10, 1987–2013. https://doi.org/10.5194/essd-10-1987-2018.

Dhital, N.B., Bhattarai, D.R., Sapkota, R.P., Rijal, K., Byanju, R.M., Yang, H.-H., 2022. Comparing the change in air quality during the COVID-19 lockdown between dry and wet seasons in Nepal. Aerosol Air Qual. Res. 22, 220201. https://doi.org/10.4209/aaqr.220201.

Dobber, M., Kleipool, Q., Dirksen, R., Levelt, P., Jaross, G., Taylor, S., Kelly, T., Flynn, L., Leppelmeier, G., Rozemeijer, N., 2008. Validation of ozone monitoring instrument level 1b data products. J. Geophys. Res. 113, D15S06. https://doi.org/10.1029/2007JD008665.

Duncan, B.N., Lamsal, L.N., Thompson, A.M., Yoshida, Y., Lu, Z., Streets, D.G., Hurwitz, M.M., Pickering, K.E., 2016. A space-based, high-resolution view of notable changes in urban NOx pollution around the world (2005–2014). Journal of Geophysical Research: Atmospheres 121, 976–996. https://doi.org/10.1002/2015JD024121.

Eil, A., Li, J., Baral, P., Saikawa, E., 2020. Dirty stacks, high stakes. Overview Brick Sector South Asia.

Filonchyk, M., Peterson, M.P., 2023. NO2 emissions from oil refineries in the Mississippi Delta. Sci. Total Environ. 898, 165569. https://doi.org/10.1016/j.scitotenv.2023.165569.

Fisher, B.L., Lamsal, L.N., Fasnacht, Z., Oman, L.D., Joiner, J., Krotkov, N.A., Choi, S., Qin, W., Yang, E.-S., 2024. Revised estimates of NO2 reductions during the COVID-19 lockdowns using updated TROPOMI NO2 retrievals and model simulations. Atmos. Environ. 326, 120459. https://doi.org/10.1016/j.atmosenv.2024.120459.

Fowler, D., Coyle, M., Skiba, U., Sutton, M.A., Cape, J.N., Reis, S., Sheppard, L.J., Jenkins, A., Grizzetti, B., Galloway, J.N., Vitousek, P., Leach, A., Bouwman, A.F., Butterbach-Bahl, K., Dentener, F., Stevenson, D., Amann, M., Voss, M., 2013. The global nitrogen cycle in the twenty-first century. Phil. Trans. Biol. Sci. 368, 20130164. https://doi.org/10.1098/rstb.2013.0164.

Galloway, J.N., Dentener, F.J., Capone, D.G., Boyer, E.W., Howarth, R.W., Seitzinger, S.P., Asner, G.P., Cleveland, C.C., Green, P.A., Holland, E.A., Karl, D.M., Michaels, A.F., Porter, J.H., Townsend, A.R., Vöosmarty, C.J., 2004. Nitrogen cycles: past, present, and future. Biogeochemistry 70, 153–226. https://doi.org/10.1007/s10533-004-0370-0.

Gurung, A., Bell, M.L., 2012. Exposure to airborne particulate matter in Kathmandu Valley, Nepal. J. Expo. Sci. Environ. Epidemiol. 22, 235–242. https://doi.org/10.1038/jes.2012.14.

Gyawali, M.S., Lamsal, L.N., Sedai, J.R., Gyawali, B., Bhattarai, K., Williams, Q., Neige, S., Sharma, S., Aryal, R., 2023. Tracking NO2 Pollution Changes Over Texas: Synthesis of In Situ and Satellite Observations. Journal of Geophysical Research: Atmospheres 128, e2022JD037473. https://doi.org/10.1029/2022JD037473.

Hofzumahaus, A., Rohrer, F., Lu, K., Bohn, B., Brauers, T., Chang, C.-C., Fuchs, H., Holland, F., Kita, K., Kondo, Y., Li, X., Lou, S., Shao, M., Zeng, L., Wahner, A., Zhang, Y., 2009. Amplified Trace Gas Removal in the Troposphere. Science 324, 1702–1704. https://doi.org/10.1126/science.1164566.

Ishtiaque, A., Shrestha, M., Chhetri, N., 2017. Rapid urban growth in the Kathmandu Valley, Nepal: monitoring land use land cover dynamics of a himalayan city with landsat imageries. Environments 4, 72. https://doi.org/10.3390/environments4040072.

Jayarathne, T., Stockwell, C.E., Bhave, P.V., Praveen, P.S., Rathnayake, C.M., Islam, M. R., Panday, A.K., Adhikari, S., Maharjan, R., Goetz, J.D., DeCarlo, P.F., Saikawa, E., Yokelson, R.J., Stone, E.A., 2018. Nepal Ambient Monitoring and Source Testing Experiment (NAMaSTE): emissions of particulate matter from wood- and dung-fueled cooking fires, garbage and crop residue burning, brick kilns, and other sources. Atmos. Chem. Phys. 18, 2259–2286. https://doi.org/10.5194/acp-18-2259-2018.

Kathmandu Post, 2022. Noise pollution affecting children in Palpa schools [WWW Document]. URL. https://kathmandupost.com/province-no-5/2022/03/12/noise-pollution-affecting-children-in-palpa-schools. accessed 2.2.24.

Kim, J., Jeong, U., Ahn, M.-H., Kim, J.H., Park, R.J., Lee, Hanlim, Song, C.H., Choi, Y.-S., Lee, K.-H., Yoo, J.-M., Jeong, M.-J., Park, S.K., Lee, K.-M., Song, C.-K., Kim, Sang-Woo, Kim, Y.J., Kim, Si-Wan, Kim, M., Go, S., Liu, X., Chance, K., Miller, C.C., Al-Saadi, J., Veihelmann, B., Bhartia, P.K., Torres, O., Abad, G.G., Haffner, D.P., Ko, D. H., Lee, S.H., Woo, J.-H., Chong, H., Park, S.S., Nicks, D., Choi, W.J., Moon, K.-J., Cho, A., Yoon, J., Kim, S., Hong, H., Lee, K., Lee, Hana, Lee, S., Choi, M., Veefkind, P., Levelt, P.F., Edwards, D.P., Kang, M., Eo, M., Bak, J., Baek, K., Kwon, H.-A., Yang, J., Park, J., Han, K.M., Kim, B.-R., Shin, H.-W., Choi, H., Lee, E., Chong, J., Cha, Y., Koo, J.-H., Irie, H., Hayashida, S., Kasai, Y., Kanaya, Y., Liu, C., Lin, J., Crawford, J.H., Carmichael, G.R., Newchurch, M.J., Lefer, B.L., Herman, J.R., Swap, R.J., Lau, A.K.H., Kurosu, T.P., Jaross, G., Ahlers, B., Dobber, M., McElroy, C. T., Choi, Y., 2020. New Era of air quality monitoring from space: geostationary environment monitoring spectrometer (GEMS). https://doi.org/10.1175/BAMS-D-18-0013.1.

Krotkov, N.A., Lamsal, L.N., Marchenko Sergey, V., Celarie, E.A., Bucsela, Eric J., Swartz, W.H., Joiner, J., 2019. OMI/Aura NO2 cloud-screened total and tropospheric column L3 global gridded 0.25 degree x 0.25 degree V3 (OMNO2d) at GES DISC. https://doi.org/10.5067/Aura/OMI/DATA3007.

Krzyzanowski, M., Apte, J.S., Bonjour, S.P., Brauer, M., Cohen, A.J., Prüss-Ustun, A.M., 2014. Air pollution in the mega-cities. Curr Envir Health Rpt 1, 185–191. https://doi.org/10.1007/s40572-014-0019-7.

Kumar, A., Dhakhwa, S., Dikshit, A.K., 2022. Comparative Evaluation of Fitness of Interpolation Techniques of ArcGIS Using Leave-One-Out Scheme for Air Quality Mapping. J geovis spat anal 6, 9. https://doi.org/10.1007/s41651-022-00102-4.

Lamsal, L.N., Duncan, B.N., Yoshida, Y., Krotkov, N.A., Pickering, K.E., Streets, D.G., Lu, Z., 2015. U.S. NO2 trends (2005–2013): EPA air quality system (AQS) data versus improved observations from the ozone monitoring instrument (OMI). Atmos. Environ. 110, 130–143. https://doi.org/10.1016/j.atmosenv.2015.03.055.

Lamsal, Lok N., Krotkov, N.A., Vasilkov, A., Marchenko, S., Qin, W., Yang, E.-S., Fasnacht, Z., Joiner, J., Choi, S., Haffner, D., Swartz, W.H., Fisher, B., Bucsela, E., 2021. Ozone Monitoring Instrument (OMI) Aura nitrogen dioxide standard product version 4.0 with improved surface and cloud treatments. Atmos. Meas. Tech. 14, 455–479. https://doi.org/10.5194/amt-14-455-2021.

Lamsal, L.N., Krotkov, N.A., Vasilkov, A., Marchenko, S., Qin, W., Yang, E.-S., Fasnacht, Z., Joiner, J., Choi, S., Haffner, D., Swartz, W.H., Fisher, B., Bucsela, E., 2021. Ozone Monitoring Instrument (OMI) Aura nitrogen dioxide standard product version 4.0 with improved surface and cloud treatments. Atmos. Meas. Tech. 14, 455–479. https://doi.org/10.5194/amt-14-455-2021.

Li, K., Jacob, D.J., Liao, H., Shen, L., Zhang, Q., Bates, K.H., 2019. Anthropogenic drivers of 2013–2017 trends in summer surface ozone in China. Proc. Natl. Acad. Sci. 116, 422–427. https://doi.org/10.1073/pnas.1812168116.

Lonsdale, C.R., Sun, K., 2023. Nitrogen oxides emissions from selected cities in north America, europe, and east Asia observed by the TROPOspheric monitoring instrument (TROPOMI) before and after the COVID-19 pandemic. Atmos. Chem. Phys. 23, 8727–8748. https://doi.org/10.5194/acp-23-8727-2023.

Mahata, K.S., Rupakheti, M., Panday, A.K., Bhardwaj, P., Naja, M., Singh, A., Mues, A., Cristofanelli, P., Pudasainee, D., Bonasoni, P., Lawrence, M.G., 2018. Observation and analysis of spatiotemporal characteristics of surface ozone and carbon monoxide at multiple sites in the Kathmandu Valley, Nepal. Atmos. Chem. Phys. 18, 14113–14132. https://doi.org/10.5194/acp-18-14113-2018.

Nepal Rastra Bank. (2021). Annual report 2019/20 (English). https://www.nrb.org.np/contents/uploads/2021/08/Annual-Report-2019-20-English.pdf.

Neupane, D., Sharma, B., Aryal, A., Acharya, S., Subedi, M., Gc, B., 2019. Detailed study of cement manufacturing industry [WWW Document]. Department of Industry. URL. https://doind.gov.np/detail/61. accessed 12.21.22.

Qu, Z., Jacob, D.J., Silvern, R.F., Shah, V., Campbell, P.C., Valin, L.C., Murray, L.T., 2021. US COVID-19 shutdown demonstrates importance of background NO2 in inferring NOx emissions from satellite NO2 observations. Geophys. Res. Lett. 48, e2021GL092783. https://doi.org/10.1029/2021GL092783.

Rimal, B., Sloan, S., Keshtkar, H., Sharma, R., Rijal, S., Shrestha, U.B., 2020. Patterns of historical and future urban expansion in Nepal. Remote Sens. 12, 628. https://doi.org/10.3390/rs12040628.

Rimal, B., Zhang, L., Stork, N., Sloan, S., Rijal, S., 2018. Urban expansion occurred at the expense of agricultural lands in the tarai region of Nepal from 1989 to 2016. Sustainability 10, 1341. https://doi.org/10.3390/su10051341.

Rupakheti, D., Adhikary, B., Praveen, P.S., Rupakheti, M., Kang, S., Mahata, K.S., Naja, M., Zhang, Q., Panday, A.K., Lawrence, M.G., 2017. Pre-monsoon air quality over Lumbini, a world heritage site along the Himalayan foothills. Atmos. Chem. Phys. 17, 11041–11063. https://doi.org/10.5194/acp-17-11041-2017.

Schumann, U., Huntrieser, H., 2007. The global lightning-induced nitrogen oxides source. Atmos. Chem. Phys. 7, 3823–3907. https://doi.org/10.5194/acp-7-3823-2007.

Stockwell, Chelsea E., Christian, T.J., Goetz, J.D., Jayarathne, T., Bhave, P.V., Praveen, P. S., Adhikari, S., Maharjan, R., DeCarlo, P.F., Stone, E.A., Saikawa, E., Blake, D.R., Simpson, I.J., Yokelson, R.J., Panday, A.K., 2016. Nepal Ambient Monitoring and Source Testing Experiment (NAMaSTE): emissions of trace gases and light-absorbing carbon from wood and dung cooking fires, garbage and crop residue burning, brick kilns, and other sources. Atmos. Chem. Phys. 16, 11043–11081. https://doi.org/10.5194/acp-16-11043-2016.

Stockwell, C.E., Christian, T.J., Goetz, J.D., Jayarathne, T., Bhave, P.V., Praveen, P.S., Adhikari, S., Maharjan, R., DeCarlo, P.F., Stone, E.A., Saikawa, E., Blake, D.R., Simpson, I.J., Yokelson, R.J., Panday, A.K., 2016. Nepal Ambient Monitoring and Source Testing Experiment (NAMaSTE): emissions of trace gases and light-absorbing carbon from wood and dung cooking fires, garbage and crop residue burning, brick kilns, and other sources. Atmos. Chem. Phys. 16, 11043–11081. https://doi.org/10.5194/acp-16-11043-2016.

Sun, K., 2022. Derivation of emissions from satellite-observed column amounts and its application to TROPOMI NO2 and CO observations. Geophys. Res. Lett. 49, e2022GL101102. https://doi.org/10.1029/2022GL101102.

Sun, K., Zhu, L., Cady-Pereira, K., Chan Miller, C., Chance, K., Clarisse, L., Coheur, P.-F., González Abad, G., Huang, G., Liu, X., Van Damme, M., Yang, K., Zondlo, M., 2018. A physics-based approach to oversample multi-satellite, multispecies observations to a common grid. Atmos. Meas. Tech. 11, 6679–6701. https://doi.org/10.5194/amt-11-6679-2018.

Thapa, R., Murayama, Y., Ale, S., 2008. City profile: Kathmandu. Cities 25, 45–57.

van Geffen, J., Boersma, K.F., Eskes, H., Sneep, M., ter Linden, M., Zara, M., Veefkind, J. P., 2020. S5P TROPOMI NO_2 slant column retrieval: method, stability, uncertainties and comparisons with OMI. Atmos. Meas. Tech. 13, 1315–1335. https://doi.org/10.5194/amt-13-1315-2020.

van Geffen, J., Eskes, H., Compernolle, S., Pinardi, G., Verhoelst, T., Lambert, J.-C., Sneep, M., ter Linden, M., Ludewig, A., Boersma, K.F., Veefkind, J.P., 2022. Sentinel-5P TROPOMI NO_2 retrieval: impact of version v2.2 improvements and comparisons with OMI and ground-based data. Atmos. Meas. Tech. 15, 2037–2060. https://doi.org/10.5194/amt-15-2037-2022.

Wang, Y., Ge, C., Garcia, L.C., Jenerette, G.D., Oikawa, P.Y., Wang, J., 2021. Improved modelling of soil NOx emissions in a high temperature agricultural region: role of background emissions on NO2 trend over the US. Environ. Res. Lett. 16, 084061. https://doi.org/10.1088/1748-9326/ac16a3.

Wei, J., Liu, S., Li, Z., Liu, C., Qin, K., Liu, X., Pinker, R.T., Dickerson, R.R., Lin, J., Boersma, K.F., Sun, L., Li, R., Xue, W., Cui, Y., Zhang, C., Wang, J., 2022. Ground-level NO2 surveillance from space across China for high resolution using interpretable spatiotemporally weighted artificial intelligence. Environ. Sci. Technol. 56, 9988–9998. https://doi.org/10.1021/acs.est.2c03834.

Weyant, C., Athalye, V., Ragavan, S., Rajarathnam, U., Lalchandani, D., Maithel, S., Baum, E., Bond, T.C., 2014. Emissions from South asian brick production. Environ. Sci. Technol. 48, 6477–6483. https://doi.org/10.1021/es500186g.

Zhong, M., Saikawa, E., Avramov, A., Chen, C., Sun, B., Ye, W., Keene, W.C., Yokelson, R. J., Jayarathne, T., Stone, E.A., Rupakheti, M., Panday, A.K., 2019. Nepal Ambient Monitoring and Source Testing Experiment (NAMaSTE): emissions of particulate matter and sulfur dioxide from vehicles and brick kilns and their impacts on air quality in the Kathmandu Valley, Nepal. Atmos. Chem. Phys. 19, 8209–8228. https://doi.org/10.5194/acp-19-8209-2019.

Zoogman, P., Liu, X., Suleiman, R.M., Pennington, W.F., Flittner, D.E., Al-Saadi, J.A., Hilton, B.B., Nicks, D.K., Newchurch, M.J., Carr, J.L., Janz, S.J., Andraschko, M.R., Arola, A., Baker, B.D., Canova, B.P., Chan Miller, C., Cohen, R.C., Davis, J.E., Dussault, M.E., Edwards, D.P., Fishman, J., Ghulam, A., González Abad, G., Grutter, M., Herman, J.R., Houck, J., Jacob, D.J., Joiner, J., Kerridge, B.J., Kim, J., Krotkov, N.A., Lamsal, L., Li, C., Lindfors, A., Martin, R.V., McElroy, C.T., McLinden, C., Natraj, V., Neil, D.O., Nowlan, C.R., O'Sullivan, E.J., Palmer, P.I., Pierce, R.B., Pippin, M.R., Saiz-Lopez, A., Spurr, R.J.D., Szykman, J.J., Torres, O., Veefkind, J.P., Veihelmann, B., Wang, H., Wang, J., Chance, K., 2017. Tropospheric emissions: monitoring of pollution (TEMPO). J. Quant. Spectrosc. Radiat. Transf. 186, 17–39. https://doi.org/10.1016/j.jqsrt.2016.05.008. Satellite Remote Sensing and Spectroscopy: Joint ACE-Odin Meeting, October 2015.